

# Research and Analysis of Optimizing Airfoil Geometry and Angle of Attack to Maximize Short Takeoff and Landing Capabilities

Jackson Wozniak

Department of Civil and Mechanical Engineering  
United States Military Academy  
West Point, NY

**Abstract**—This paper will examine the aerodynamic properties of two airfoils with different angles of attack in order to optimize short takeoff and landing (STOL) capabilities. The lift, drag, and pressure coefficients will be simulated and compared to experimental values. This analysis will be conducted using Computational Fluid Dynamics (CFD) and experimental wind tunnel data collected by the National Advisory Committee for Aeronautics (NACA). This study compares the NACA 2412 and the NACA 4412 at angles of attack between -18 and 18 degrees. The objective of the study is to optimize the lift coefficient which in turn provides aircraft with the lift force required to minimize required takeoff distance. The results showed that using a high-quality mesh provided valuable data in close agreement with experimental values. The CFD simulations provide useful data that supplement experimental methods and reduce dependency on conducting wind tunnel testing.

**Keywords**—Computational Fluid Dynamics, Angle of Attack, Short Takeoff and Landing, Lift Coefficient, Drag Coefficient, Pressure Coefficient, Bernoulli's Principle.

## I. INTRODUCTION

Military pilots often need to operate in austere conditions to accomplish the mission. This includes unideal conditions for takeoff and landing such as short runways and other short takeoff/landing spaces. Short Takeoff and Landing (STOL) Aircraft are aircraft capable of taking off and landing on a short runway or takeoff/landing space. To take off under these conditions, it is important to maximize lift force, so this study will attempt to find an optimal lift coefficient.

## II. BACKGROUND

### A. Airfoil Geometry

An airfoil is a cross section of a body within a fluid flow that produces an aerodynamic force. The leading edge of an airfoil is the point at the front with maximum curvature. The trailing edge is the point at the rear containing minimum curvature. The chord line is the straight line joining the leading edge and the trailing edge. The camber line divides the upper and lower half of an airfoil equally. The angle of attack is the angle between the chord line and the fluid flow stream.

The National Advisory Committee for Aeronautics developed numerous airfoils which are used for different aircraft. NACA airfoils follow the nomenclature NACA MPXX where M, P, and XX represent different geometric properties. M is the

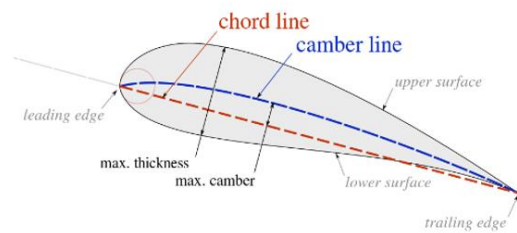


Figure 1: Geometry of an Airfoil

magnitude of the maximum camber position as the percentage of chord length. P is the position of the maximum camber from the airfoil's leading edge and is given in tenths of the chord. XX provides the maximum thickness of the airfoil as a percentage of the chord length. For example, a NACA 2412 has a maximum camber of 2% of the chord length, a maximum camber located at 40% of the chord length (from the leading edge), and a maximum thickness of 12% of the chord length.

### B. Lift and Drag Analytical Solutions

As an airfoil moves through air, air exerts both lift and drag force on the airfoil. Lift and drag forces are caused by wall shear stresses and pressure stresses. Wall shear stresses occur tangential to the airfoil's surface, and pressure stresses occur normal to the surface. The lift and drag coefficients are valuable components of the lift and drag forces. The lifting force generated by an airfoil depends on density and relative velocity. The force is also dependent on airfoil shape, angle of attack, and air density; these three variables are embedded in the lift coefficient. Thus, the lift equation is

$$L = \frac{1}{2} \rho U^2 S C_L \quad (1)$$

Where L is the lifting force,  $\rho$  is the air density, U is the relative velocity, S is the planform area of the airfoil, and  $C_L$  is the lift coefficient.<sup>1</sup> Similarly, the drag force can be calculated by the equation

$$D = \frac{1}{2} \rho U^2 S C_D \quad (2)$$

Where  $D$  is the drag force,  $\rho$  is the air density,  $U$  is the relative velocity,  $S$  is the area of the airfoil, and  $C_D$  is the drag coefficient.<sup>1</sup>

### C. Bernoulli's Principle

The pressure distribution around an airfoil determines the lift and drag forces. The pressure difference among different airfoils within different boundary conditions stems from Bernoulli's Principle. For any two points in an irrotational flow field,

$$p + \frac{1}{2} \rho V^2 = \text{const} \quad (3)$$

Where  $p$  is pressure,  $\rho$  is density, and  $V$  is the velocity. The physical significance of Bernoulli's Principle is that as velocity increases, pressure decreases, and as velocity decreases, pressure increases.<sup>2</sup> Bernoulli's Principle illustrates how the velocity of fluid can generate lift. For instance, note in Figure 2 that the leading edge of the airfoil contains a stagnation point where the velocity is equal to zero. The fluid flow is diverted into one segment above the airfoil and one segment below the airfoil. Above the airfoil, the flow is pinched together and flows faster than the flow below the airfoil. This is evident in the velocity magnitude contour plot and the streamlines displayed in Figure 2 and Figure 3, respectively. Considering Bernoulli's Principle, the airfoil will have low pressure on the top and high pressure on the bottom. This pressure differential causes a lift force.

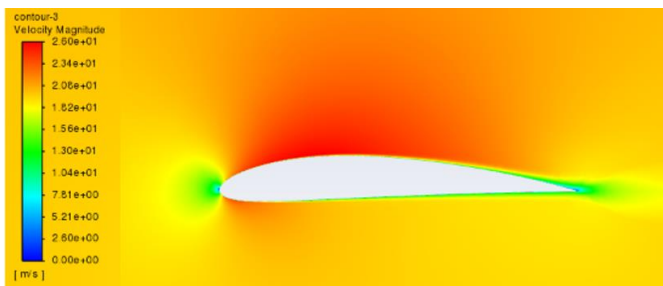


Figure 2: Velocity Magnitude Contour Plot of a NACA 4412 Airfoil

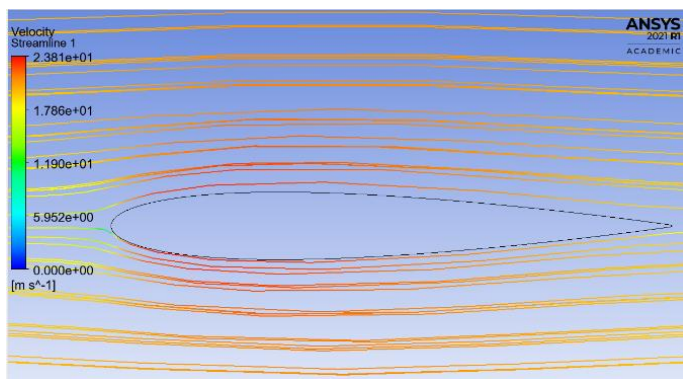


Figure 3: Velocity Streamlines over a NACA 2412 Airfoil

### D. The Spalart-Allmaras Turbulence Model

Turbulence models are mathematical models that predict the air's turbulence effects. These complex equations are often designed for specific applications. This study utilized the Spalart-Allmaras Turbulence Model which was developed primarily for aerodynamic flow over an airfoil. The Spalart-Allmaras Model is an Eddy viscosity transport model. Eddy viscosity is the internal friction between fluid particles which are moving randomly. It depends on fluid density, and it relates the average shear stress (stress acting parallel to the area) and the vertical velocity component. This model is effective for modeling fluid flow within wall-bounded volumes, so it was an effective method for simulating turbulence within a virtual wind tunnel.

## III. MODELING AND SIMULATION

### A. Methodology

Computational Fluid Dynamics (CFD) is an efficient method of solving physical problems in accordance with the equations of fluid motion. This method is economical in aerospace problems because it saves the costs of running experimental wind tunnel tests. This study will conduct a 2D analysis on the airfoils using ANSYS Fluent. The first step of running the simulation is sketching the 2D airfoil by utilizing an airfoil plotter. The plotter on [airfoiltools.com](http://airfoiltools.com) allows the user to specify chord, radius, and thickness to create an airfoil. The plotter also has pre-loaded NACA airfoils. The airfoil can be saved as a list of coordinates and inputted into ANSYS to create the airfoil surface. Next, a closed volume geometry was created to simulate a wind tunnel. This volume, shown in Figure 4, is created as a semicircle connected to a rectangle. Following this, I created the Boolean which creates a surface between the flow system and the airfoil. After creating this, the system must be meshed. The mesh is a significant part of the simulation because the finer the mesh is, the more accurate the simulation is. The mesh is divided into many cells, and the governing equations will be solved at every cell. Therefore, around the edge of the airfoil, the mesh will be finer than in other parts throughout the flow domain to understand the aerodynamic behavior along the airfoil. This study accomplishes this through adding ten layers of cells around the airfoil with each layer containing 250 cells, shown in Figure 5.

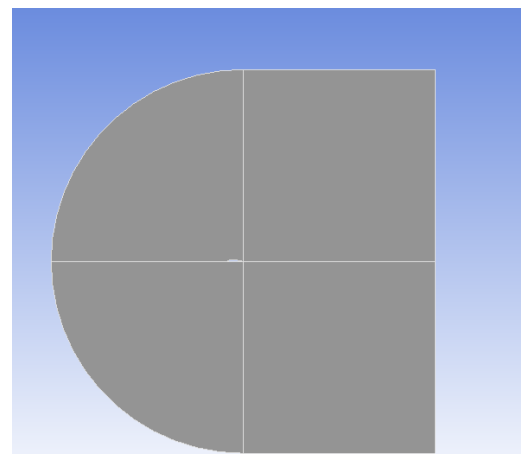


Figure 4: Physical Domain

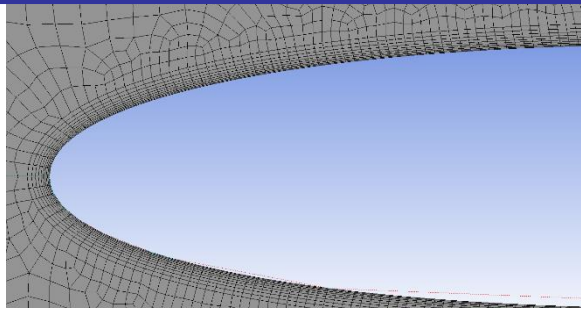


Figure 5: Mesh around the NACA 2412 Airfoil

**B. Physical Domain and Boundary Conditions**

This study used an enclosed volume containing a semicircle and a rectangular shape. I divided the volume into four quadrants. This step was useful for meshing a C-shaped mesh along the left half of the enclosed volume. The outer edge along the semicircle is the inlet. The outer edge along the right half of the rectangle will be the pressure outlet. This paper’s primary focus is the lift coefficient, so I will be using a velocity comparable to a reasonable takeoff speed of 20m/s or around 40 knots. The components of the fluid flow velocity are varied in order to obtain different angles of attack. For instance, to simulate a 6° angle of attack, the x and y components of the fluid flow velocity are  $20\cos(6^\circ)$  and  $20\sin(6^\circ)$ , respectively. This study considers a second order upwind scheme for the modified turbulent viscosity method. This method computes higher-order accuracy at cell faces through using a Taylor series expansion.<sup>5</sup>

Table 1: Operating Parameters

Variable	Condition
Viscous Model	Spalart-Allmaras Model
Fluid	Air
Density	1.225 kg/m <sup>3</sup>
Viscosity	1.7894*10 <sup>-5</sup>
Velocity Magnitude	20 m/s
Reynold’s Number	600,000
Temperature	288.16 K
Modified Turbulent Viscosity Method	Second Order Upwind

**C. Verification**

Verification is a valuable step in CFD that determines if the implementation of the governing equations is correct. Results can be verified by comparing results with analytic results or other simulations. The comparison in verifying the data will be comparing the pressure coefficient plot in the pre-stall region with another study and with expected trends. The pressure coefficient plot demonstrates consistency with the plot obtained in [6].

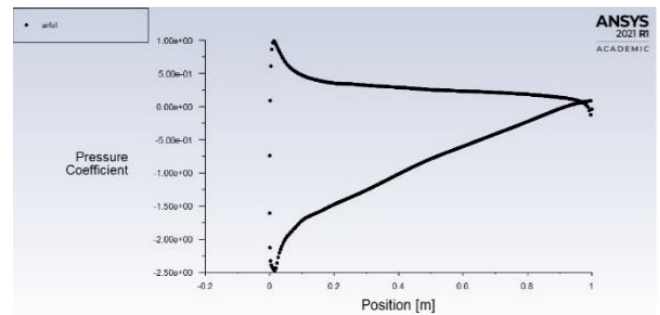


Figure 6: Pressure Coefficient Plot of a NACA 4412 Airfoil at an 8° Angle of Attack

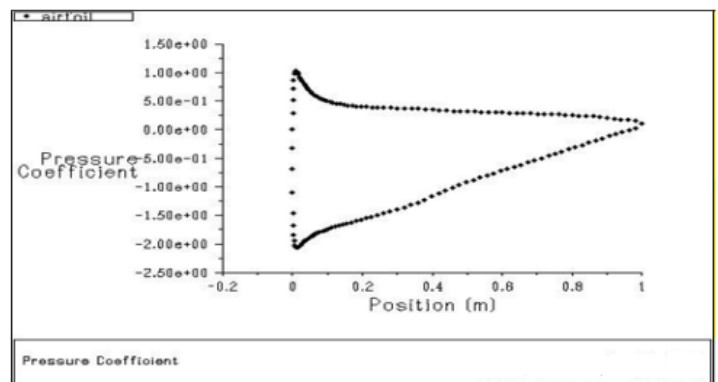


Figure 7: Pressure Coefficient Plot of a NACA 4412 at an 8° Angle of Attack<sup>6</sup>

**D. Validation**

Validation is another important step in the simulation process and determines if the simulated results agree with physical reality. The results show agreement with this principle. The contour plot has clearly defined low pressure contours above the airfoil. Further, the leading edge contains a point of high pressure illustrating the point before the fluid flow divides into two flows. The pressure distribution of the NACA 4412 is consistent with the known properties of airfoil pressure. Another effective method to validate the data is to compare the obtained numerical lift coefficients with the velocity magnitude contour plot during a stall. Valid data will reflect that the angle of attack providing a maximum lift coefficient corresponds to the stall angle. Further, at the stall angle, the air begins to separate from the wing. Table 2 and Figure 8 demonstrate consistency with the known properties of stalls in physical reality. The pressure and velocity contour plots for the NACA 2412 are in the appendix and also obey these properties.

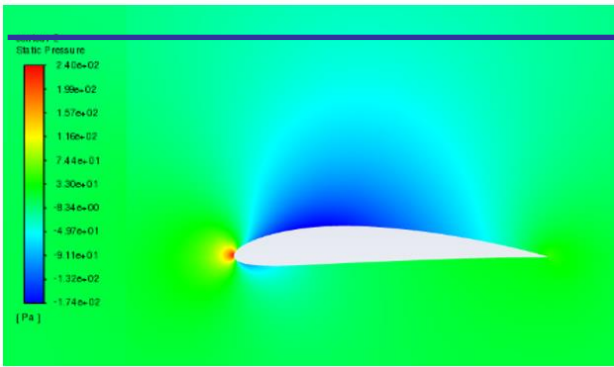


Figure 7: Pressure Contour Plot of a NACA 4412 With a 0° Angle of Attack

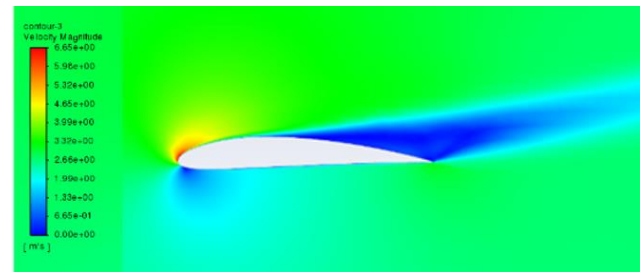


Figure 8: Velocity Magnitude Contour Plot of a NACA 4412 With a 16° Angle of Attack

Table 2: Angle of Attack and Lift Coefficients for a NACA 4412

Angle of Attack	Lift Coefficient
6°	0.97893
8°	1.1552
10°	1.3145
12°	1.4446
14°	1.5181
16°	1.5257
18°	1.4375

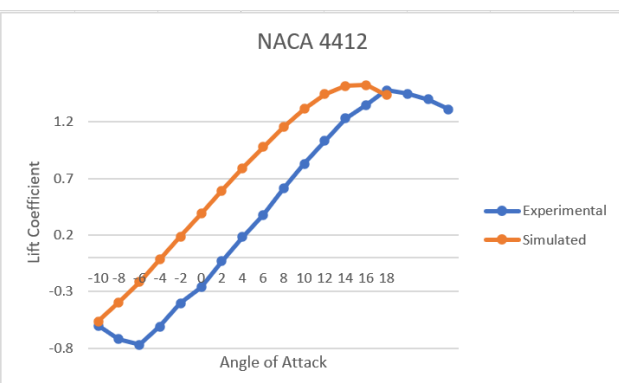


Figure 9: NACA 4412 Lift Coefficient Values

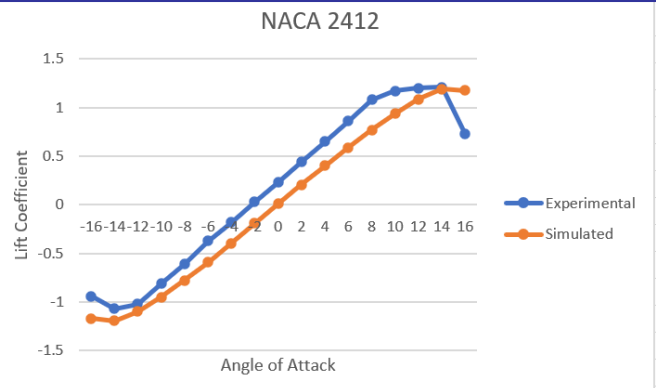


Figure 10: NACA 2412 Lift Coefficient Values

#### IV. RESULTS AND DISCUSSION

The data provide useful insight regarding the maximum lift coefficient, or the lift coefficient obtained during a stall. These results provide not only data about the given airfoils, but they also provide information on the combination of parameters that optimizes the lift coefficient. For instance, the NACA 4412 has the greatest lift coefficient which corresponds to the greatest lift force. The only geometric parameter that differs between the NACA 2412 and the NACA 4412 is the maximum camber position which is denoted by the first digit in the NACA 4412. This data point suggests that the maximum camber position of 4% of the chord length is best coupled with a thickness of 12% of the chord length. The data support that an optimal airfoil geometry contains a maximum camber position of 4% of the chord length and a thickness of 12% of the chord.

#### V. CONCLUSIONS AND FUTURE WORK

In conclusion, the lift coefficient is optimized by the NACA 4412. The combination of a larger maximum camber position coupled with a 12% thickness value provided the airfoil with the optimal lift coefficient value. The CFD simulations overall provided reasonably close agreement with the experimental wind tunnel test data. The NACA 2412 and NACA 4412 simulations were within 2% and 3% of the experimental values, respectively. The simulations verified the fundamental aerodynamic properties of physical reality. The top of the airfoil undergoes a low pressure and a high velocity while the bottom of the airfoil undergoes a high pressure and a low velocity.

In future work, further study of the lift coefficient for different airfoils will provide useful knowledge about STOL aircraft. Additionally, conducting a study on the lift/drag ratio will be paramount to maximizing STOL capabilities. This will provide a more accurate assessment of lift coefficient and will allow for analysis of landing capabilities.



ACKNOWLEDGMENT

I express my gratitude to Mr. John Pegues for advising my studies over the course of this research project. I would also like to thank Dr. Ted. Hromadka and Dr. Nicholas Wimer for using their CFD expertise to assist me in conducting these simulations.

A. Figures and Tables

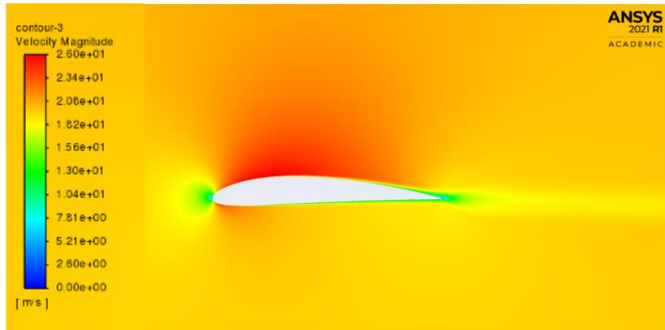


Figure 1: Velocity Magnitude Contour Plot for a NACA 2412 With a 0° Angle of Attack

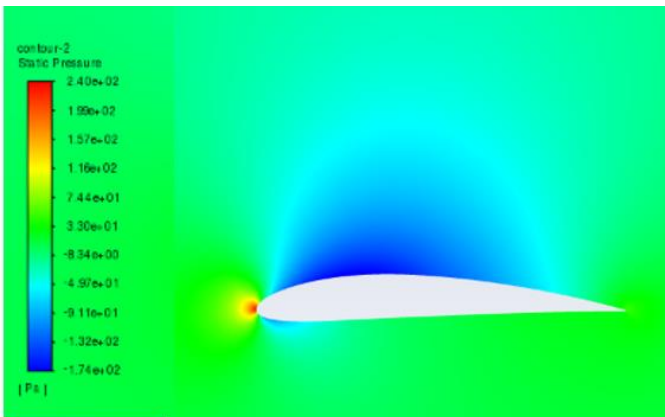


Figure 2: Pressure Contour Plot for a NACA 2412 With a 0° Angle of Attack

Table 1: Maximum Lift Coefficients

	NACA 2412	NACA 4412
Maximum Simulated Lift Coefficient	1.191	1.5257
Maximum Experimental Lift Coefficient	1.21	1.48

Table 2: NACA 4412 Lift Coefficients

Angle of Attack	Experimental	Simulated
-10°	-0.61	-0.56299
-8°	-0.4	-0.39456
-6°	-0.26	-0.21304
-4°	-0.03	-0.015978
-2°	0.185	0.18508
0°	0.38	0.38894
2°	0.61	0.59153
4°	0.83	0.79107
6°	1.03	0.97893
8°	1.23	1.1552
10°	1.35	1.3145
12°	1.48	1.4446
14°	1.45	1.5181
16°	1.4	1.5257
18°	1.31	1.4375

Table 3: NACA 2412 Lift Coefficients

Angle of Attack	Experimental	Simulated
-16	-0.94	-1.1673
-14	-1.07	-1.1916
-12	-1.02	-1.0955
-10	-0.81	-0.94925
-8	-0.61	-0.77669
-6	-0.37	-0.58983
-4	-0.18	-0.3941
-2	0.03	-0.19162
0	0.23	0.009265
2	0.44	0.20751
4	0.65	0.40382
6	0.86	0.59064
8	1.08	0.77031
10	1.17	0.93963
12	1.2	1.0872
14	1.21	1.191
16	0.73	1.1762

#### REFERENCES

- [1] Abbott, Ira H., "Theory of Wing Sections," pp. 3, 478-479, 488-489.
- [2] Anderson, John D. Jr., "Fundamentals of Aerodynamics," 210.
- [3] Coiro, D. P., A. de Marco, F. Nicolosi, N. Genito, and S. Figliolia, "Design of a Low-Cost Easy-to-Fly STOL Ultralight Aircraft in Composite Material." Czech Technical University in Prague, Acta Polytechnica, Vol. 45 No. 4/2005.
- [4] Kandwal, S and Dr. S. Singh, "Computational Fluid Dynamics Study of Fluid Flow and Aerodynamic Forces on An Airfoil."
- [5] "18.3.1 Spatial Discretization," ANSYS, [afs.ansys.com](http://www.ansys.com).
- [6] Madhukeshwara, Ravi H.C., and S. Kumarappa, "Numerical Investigation of Flow Transition for NACA-4412 Airfoil Using Computational Fluid Dynamics."
- [7] NACA 4 Digit Airfoil Generator, Airfoil Tools.
- [8] Mullen, Benjamin, "Flow Over an Airfoil," Cornell University.
- [9] Sahin, Izzet and Adem Acir, "Numerical and Experimental Investigations of Lift and Drag Performances of NACA 0015 Wind Turbine Airfoil," International Journal of Materials, Mechanics and Manufacturing, Vol. 3, No. 1, February 2015.